

Functional graphene nanoflakes/cyanate/epoxy nanocomposites: mechanical, dielectric and thermal properties

Juan Ding¹ · Ying Huang¹ · Tiaozheng Han¹

Received: 3 December 2014 / Accepted: 21 November 2015 / Published online: 7 December 2015
© Iran Polymer and Petrochemical Institute 2015

Abstract Functional graphene nanoflakes/cyanate/epoxy (FGNs/CE/EP) nanocomposites were prepared with solution insertion method. The functional graphene nanoflakes (FGNs) were added to CE/EP copolymer to improve the integrated properties of the FGNs/CE/EP nanocomposites. The non-isothermal behavior of the FGNs/CE/EP nanocomposites was investigated using differential scanning calorimetry at different heating rates. The result clearly indicated that the functional graphene nanoflakes (FGNs) acted as a catalyst over the whole curing process and shortened the curing time. The mechanical, dielectric and thermal properties were characterized via mechanical, dielectric and thermogravimetric analysis (TGA) techniques, respectively. The results showed that the mechanical properties of the nanocomposites, enhanced with 2.0 wt% FGNs, not only because the flexural strength reached the optimum value, but also because the impact strength acquired the best value. When compared with the dielectric properties of the CE/EP copolymer, the dielectric constant and dielectric loss factor of the FGNs/CE/EP nanocomposites with 2.0 wt% of FGNs slightly increased. The TGA of the nanocomposites was thoroughly recorded, which indicated that the thermal properties of the FGNs/CE/EP nanocomposites increased as well. Therefore, the FGNs acted as a catalyst as well as a reinforcing agent in the FGNs/CE/EP nanocomposites.

Keywords Bisphenol A dicyanate ester · Bisphenol A epoxy · Functional graphene nanoflakes · Nanocomposites · Dielectric properties · Thermal properties

Introduction

Graphene, a monolayer with sp^2 -bonded carbon atoms arranged in a honeycomb lattice, has attracted much attention since the first report of its successful separation from graphite by Novoselov et al. in 2004 [1]. It is the thinnest and hardest nanomaterial in the world [2, 3]. Because of its individual nanostructures and remarkable physical and chemical properties [4, 5], it has been considered as a filler candidate to improve the integrated properties of polymers [6]. The nanomaterials, such as layered clay silicate (montmorillonite) [7, 8], SiC [9], SiO₂ [10], and carbon nanotubes (CNTs) nanoparticles [11, 12], etc., were investigated according to the literature in the previous works. Interestingly, graphene and its derivatives are frequently used in polymers, such as, poly (methyl methacrylate) (PMMA) [13], polyurethane (PU) [14], polyamide (PA) [15], polystyrene (PS) [16], polypropylene (PP) [17], bismaleimide [18–20], epoxy [21–23], cyanate ester [24, 25] and so on. However, two problems with the polymers prevail which are as follows: (1) graphene is hard to disperse uniformly in the matrices; (2) the interfacial bonding between graphene and matrices is weak. Therefore, it is necessary to explore the effective methods for graphene functionalization [26, 27].

In this study, cyanate ester (CE) resin was selected as the basic matrix because it has remarkable properties, such as good dielectric [28–30] and mechanical properties [31], excellent thermal stability [32, 33] and good processing characteristics [34], thus it can be a good alternative to other thermosetting resins used in the fields of aviation

✉ Ying Huang
yingh@nwpu.edu.cn

¹ Department of Applied Chemistry, The Key Laboratory of Space Applied Physics and Chemistry, Ministry of Education, School of Science, Northwestern Polytechnical University, Xi'an 710072, People's Republic of China

and aerospace, microelectronics, surface mount technology (SMT) and electronic printed circuit board (PCB), etc.

In this work, the functional graphene nanoflakes (FGNs) were prepared by chemical method. The FGNs/CE/EP nanocomposites were prepared via solution intercalation method, and then the comprehensive properties of the nanocomposites were investigated.

Experimental

Materials

Bisphenol A dicyanate (BADCy) ester, a white crystal powder, (purity $\geq 99\%$, cyanate equivalent of 139 g/eq), was purchased from Jiangdu Wuqiao Resin Factory (Yangzhou, China). Bisphenol A epoxy resin, (viscosity: 12,000–15,000 cp, EEW: 0.51), a colorless, transparent and syrupy liquid, was obtained from Xi'an Resin Factory (Xi'an, China). Natural graphene flakes were provided by Xinghe Graphite Co., Ltd., (Qingdao, China). γ -(2,3-Epoxypropoxy) propyltrimethoxysilane was purchased from Sinopharm Chemical Reagent Co., Ltd., (Xi'an, China). The potassium permanganate (KMnO_4), sulfuric acid (H_2SO_4 , 98%), absolute ethyl alcohol and acetone were obtained from Xi'an Chemical Reagent Factory (Xi'an, China).

Preparation of graphene oxide (GO)

Graphene oxide (GO) was synthesized from natural graphene through Hummers' method according to the literature procedure [35]. The steps were as follows: 3.0 g natural graphite flakes, 3.0 g NaNO_3 and 147 mL concentrated H_2SO_4 were mixed with stirring in an ice-water bath. Then, 18 g KMnO_4 was added into the mixture slowly. In the next step, the solution was stirred for 3 h at 35 °C to form a thick paste. Deionized water of 120 mL was injected into the thick paste slowly and the resulting solution was stirred for 30 min while the temperature increased to 85 °C. Finally, 750 mL deionized water containing 30 mL H_2O_2 was added until the color turned into brownish yellow, followed by filtering the solution before cooling. After that, the filter cake was washed with deionized water several times until its pH was neutral and dried in a vacuum oven at 60 °C for 24 h. The GO was sealed and stored at room temperature for further use.

Preparation of the functional graphene nanoflakes (FGNs)

100 mg GO was heated in a tube furnace at 1050 °C for 30 s, and then cooled at room temperature. The resultant product was denoted as graphene (GN).

100 mg GN was dispersed in 100 mL absolute ethyl alcohol (1 mg/mL), and sonicated for 1 h. Next, 10 mL of 95% ethanol solution with 0.5 g γ -(2,3-epoxypropoxy) propyltrimethoxysilane was added slowly with continuous stirring at 65 °C for 24 h. Finally, deionized water was used to filter and wash the filter cake several times to remove the unreacted coupling agent. The filter cake was dried in an oven to obtain functional graphene nanoflakes, denoted as FGNs. Then, xFGNs ($x = 0.5, 1.0, 2.0, \text{ and } 3.0 \text{ wt}\%$) were dispersed in acetone (1 mg/mL) and sonicated for 5 h for further use.

Preparation of CE/EP copolymer

The cyanate ester (CE) monomer was stirred at 130 °C for 1 h, and then appropriate epoxy (EP) was incorporated into the liquid and stirred at 100 °C for 2 h to form a homogeneous prepolymer, which was denoted as CE/EP prepolymer. After that, the mixture was degassed to remove entrapped air at 100 °C for 30 min in a vacuum oven. Finally, the mixture was poured into a mold, the inner surface of which was coated with Teflon release paper. The cure and post-cure processes followed the protocol: 180 °C/2 h + 200 °C/6 h and 220 °C/4 h, successively.

Preparation of FGNs/CE/EP nanocomposites

The pre-weighed xFGNs were added into the CE/EP prepolymer, prepared according to the above procedure, and stirred at 100 °C for 1 h. The residual acetone was evaporated with vacuum distillation. The mixture was degassed to remove entrapped air at 100 °C for 30 min in a vacuum oven, and then the mixture was poured into a mold, the inner surface of which was coated with Teflon release paper. The cure and post-cure processes followed the protocol: 180 °C/2 h + 200 °C/6 h, and 220 °C/4 h, successively.

Characterizations and measurements

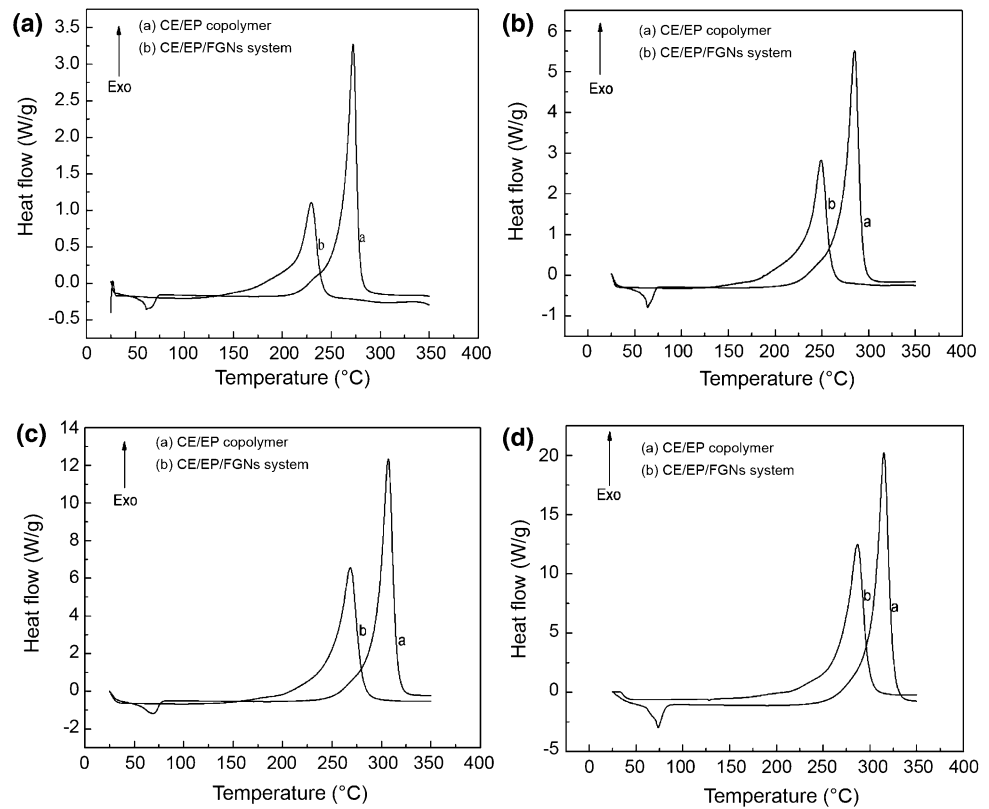
Differential scanning calorimeter (DSC)

Differential scanning calorimeter (DSC) 700 (A Mettler Toledo Instruments, Switzerland) was used to character the prepolymer. Each sample weighed 5–10 mg and was placed in sealed aluminum crucible under N_2 atmosphere at a 60 mL/min flow rate. The samples for non-isothermal scans were heated from room temperature to 350 °C at different heating rates of 5, 10, 20, and 30 °C/min, respectively.

Mechanical properties

The mechanical properties of the samples including unnotched impact (Izod) and flexural strength were tested using an

Fig. 1 The comparison of DSC curves between the CE/EP and the CE/EP/FGNs prepolymers at different heating rates, **a** 5 °C/min, **b** 10 °C/min, **c** 20 °C/min and **d** 30 °C/min



Instron Universal Testing Apparatus (USA), according to GB/T2571-1995 and GB/T2570-1995 and the dimensions of impact and flexural test specimens were $80 \times 10 \times 4 \text{ mm}^3$ and $80 \times 15 \times 4 \text{ mm}^3$, respectively. Meanwhile, at least five samples needed to be prepared for each measurement.

Scanning electron microscopy

The flexural and impact fractured surfaces of the specimens were observed using a Quanta 200 SEM (USA) at an accelerated voltage of 20 kV. All the specimens were dried at 65 °C for 24 h, and then they were coated with a thin layer of Au for SEM imaging.

Dielectric properties

The dielectric properties of the specimens were tested with a S914 broadband dielectric loss spectrometer (QBG-3D, China). Each specimen had the thickness of 2 mm and diameter of 27 mm.

Thermogravimetry analysis (TGA)

Thermal analysis of the specimens was performed with a Q50 TGA (TA Instrument Co., USA) from room temperature to 800 °C with heating rate of 20 °C/min, in N_2 atmosphere.

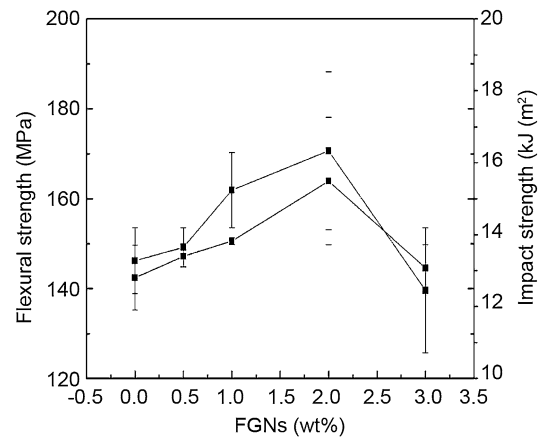


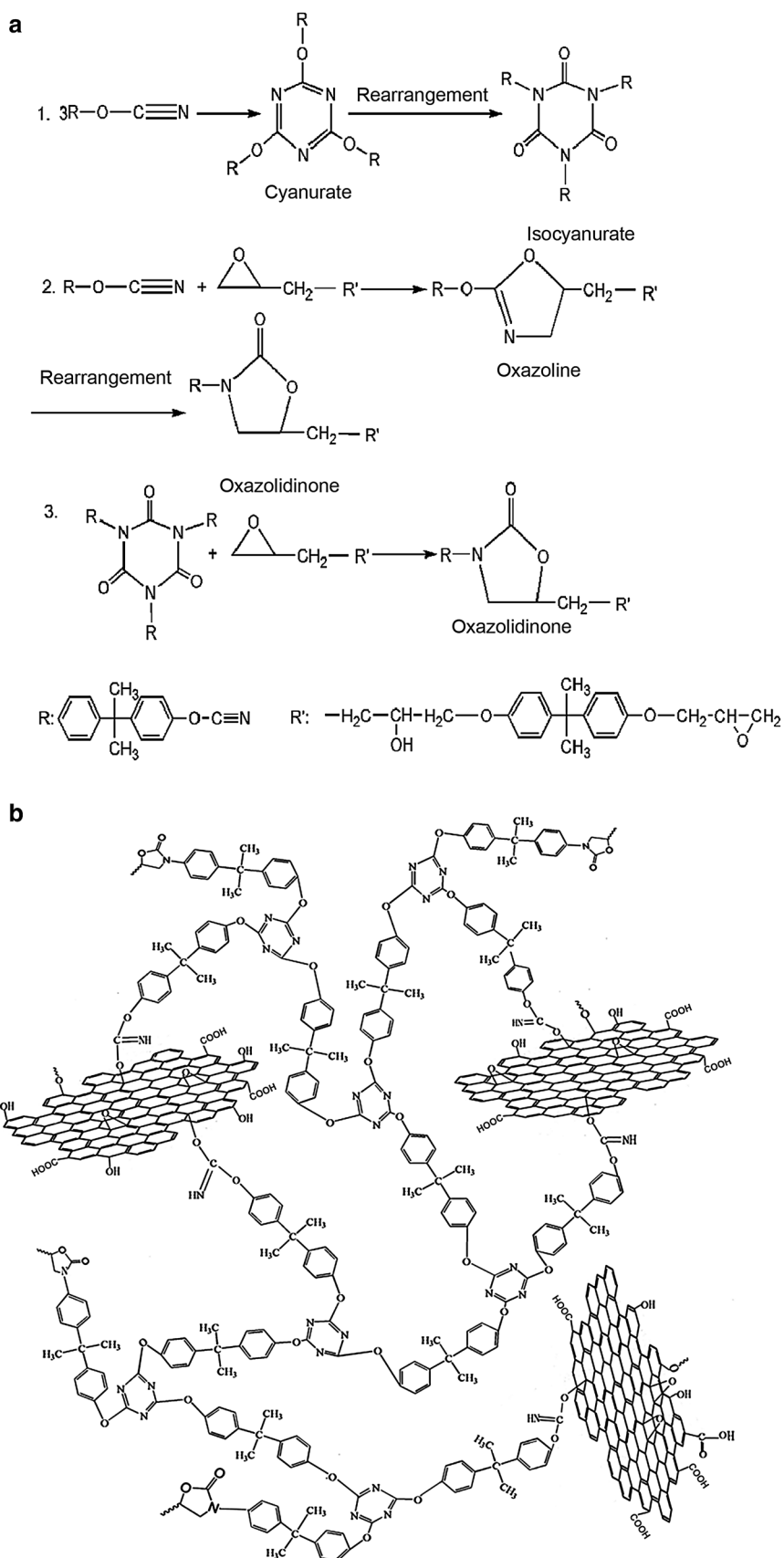
Fig. 2 Mechanical properties of FGNs/CE/EP nanocomposites

Results and discussion

Dynamic DSC analysis

Figure 1 presents the detail of non-isothermal DSC curves including the CE/EP and CE/EP/FGNs prepolymers at the heating rates of 5, 10, 20, and 30 °C/min, respectively. The exothermic peaks are upwards. In Fig. 1, the temperatures corresponding to the peak of CE/EP/FGNs prepolymer are lower than those of CE/EP at the same heating rate. The

Scheme 1 The reaction mechanism of CE and EP as well as the structure of the FGNs/CE/EP nanocomposites **a** the reaction mechanism of CE and EP and **b** the structure of the FGNs/CE/EP nanocomposites



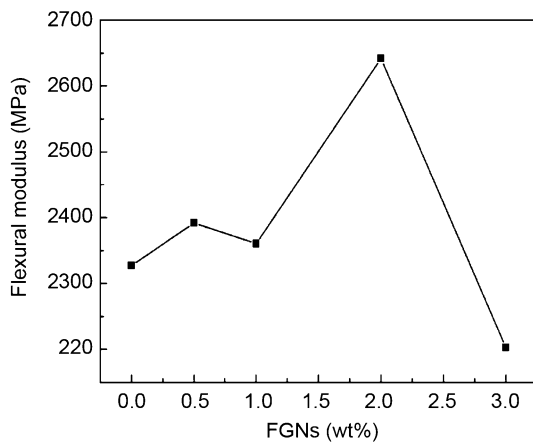


Fig. 3 Variation in flexural modulus versus the FGNs content

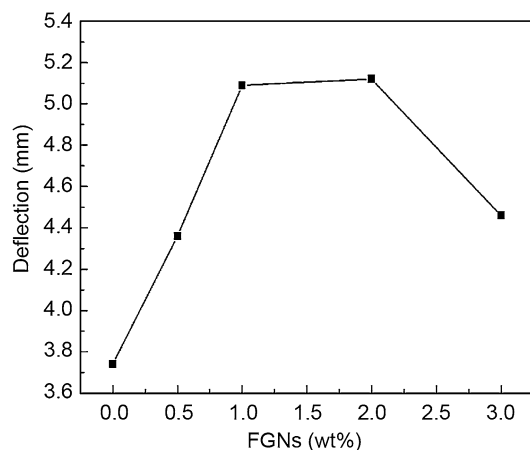


Fig. 4 Variation in deflection versus the FGNs content

result of the comparison clearly indicates that the FGNs have catalytic effect on the curing process of the CE/EP/FGNs prepolymer.

Mechanical properties of the FGNs/CE/EP nanocomposites

The mechanical properties of the FGNs/CE/EP nanocomposites with various FGNs contents are shown in Fig. 2. It can be seen that the flexural and impact strength increase in the initial phase. The flexural and impact strength with 2.0 wt% FGNs reach up to the maximum values, 170.8 MPa and 15.5 kJ/m², i.e., by 1.17 times and 1.21 times, respectively. However, the curves slightly decrease by further increasing of the FGNs content. It is believed that the incorporation of appropriate FGNs content in the FGNs/CE/EP nanocomposites improves their mechanical properties. A detail polymerization mechanism analysis conducted to examine the results is that: the silane coupling

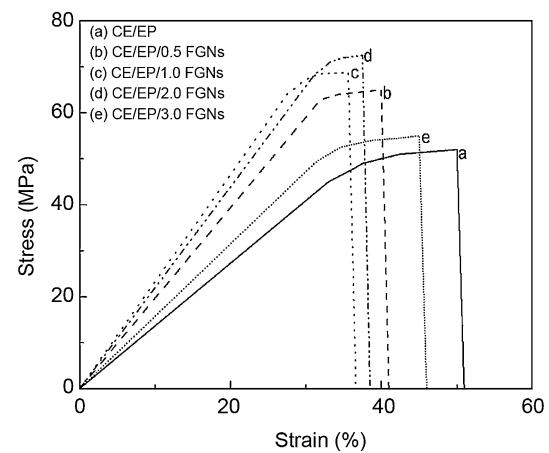


Fig. 5 Stress–strain curves

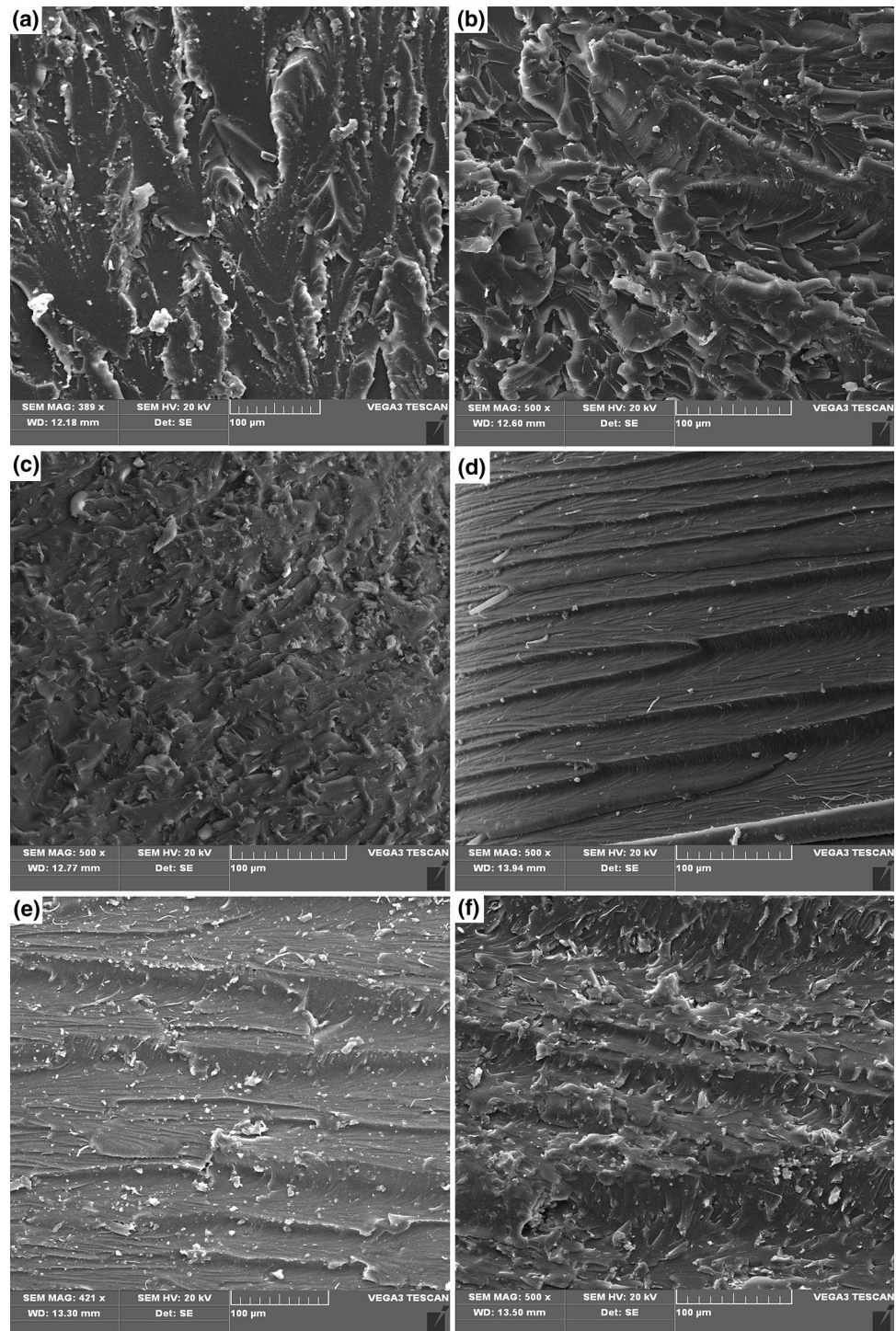
agent, as a “bridge” group, can react with the hydroxyls of the graphene surface and isocyanate groups of the matrix, forming strong interfacial bonding between different components [36]. The reaction mechanism of the CE and EP as well as the structure of the nanocomposites is shown in Scheme 1, respectively.

The variation of the flexural modulus versus the content of FGNs and the variation of deflection versus the content of FGNs at break are shown in Figs. 3 and 4, respectively. It can be seen that for the FGNs/CE/EP nanocomposites, the flexural modulus and deflection achieve the maximum value with 2.0 wt% FGNs content, corresponding to the result of the flexural strength in Fig. 2. Figure 5 shows the strain–stress curves of the FGNs/CE/EP nanocomposites at various FGNs contents. From Fig. 5, it can be seen that for the FGNs/CE/EP nanocomposites, the stress-at-break increases with the FGNs content (2.0 wt% FGNs), while the strain-at-break decreases initially and then it increases with increasing the FGNs content.

SEM micrographs of the FGNs/CE/EP nanocomposites

Typical images of the flexural and impact fracture surfaces on the FGNs/CE/EP nanocomposites with different FGNs contents are displayed in Fig. 6. The flexural fracture surfaces of the FGNs/CE/EP nanocomposites with 0, 1.0 and 3.0 wt% FGNs contents are shown in Fig. 6a–c, respectively. The impact fracture surfaces of the FGNs/CE/EP nanocomposites with 0, 1.0 and 3.0 wt% FGNs contents are shown in Fig. 6d–f, respectively. The CE/EP copolymer exhibits river, tongue and scales patterns (Fig. 6a, d), suggesting a typical brittle feature. Meanwhile, rougher surfaces are observed in the fracture surfaces of the FGNs/CE/EP nanocomposites with various FGNs contents. Dimple zones like sea waves, smaller scales and fibrous patterns are observed in the fracture surfaces of the FGNs/CE/EP

Fig. 6 SEM images of the flexural fracture surfaces and the impact fracture surfaces corresponding to the FGN/CE/EP system with various FGNs contents. Flexural fracture surfaces: **a** 0 wt% FGNs, **b** 1.0 wt% FGNs and **c** 3.0 wt% FGNs; Impact fracture surfaces: **d** 0 wt% FGNs, **e** 1.0 wt% FGNs and **f** 3.0 wt% FGNs



nanocomposites, indicating that the fracture surfaces have a typical tough feature.

Dielectric properties of the FGNs/CE/EP nanocomposites

It is well known that the remarkable dielectric property is one of the most desirable properties for the cyanate

resin and its derivatives. The dielectric properties of the FGNs/CE/EP nanocomposites are shown in Fig. 7. For the FGNs/CE/EP nanocomposites, the dielectric constant increases and the dielectric loss factor enhances significantly with 2.0 wt% FGNs content. The reasons are that the dielectric loss of the FGNs and the interface polarization between the FGNs and the matrix are large.

Fig. 7 Dielectric constant and dielectric loss of the FGNs/CE/EP nanocomposites with different FGNs content from 10 to 60 MHz, respectively; **a** dielectric constant versus FGNs content and **b** dielectric loss versus FGNs content

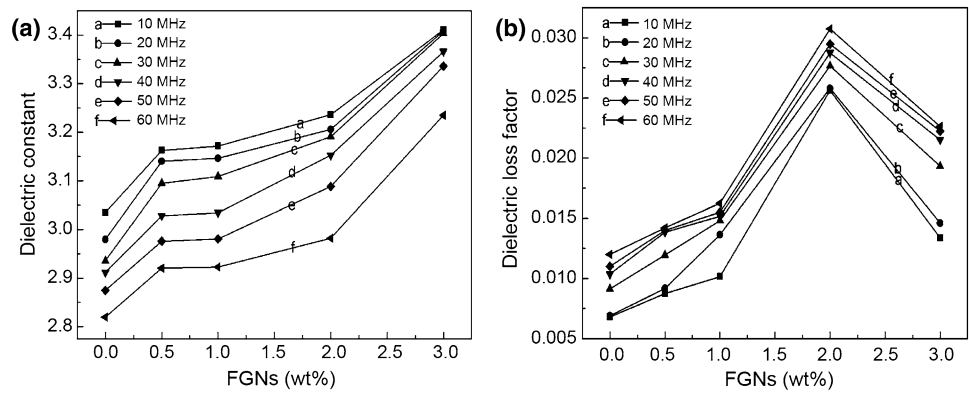


Fig. 8 TG-DTG curves of pure CE resin, CE/EP copolymer and the CE/EP/xFGNs system ($x = 0.5, 1.0, 2.0,$ and 3.0 wt%); **a** TG curves and **b** DTG curves

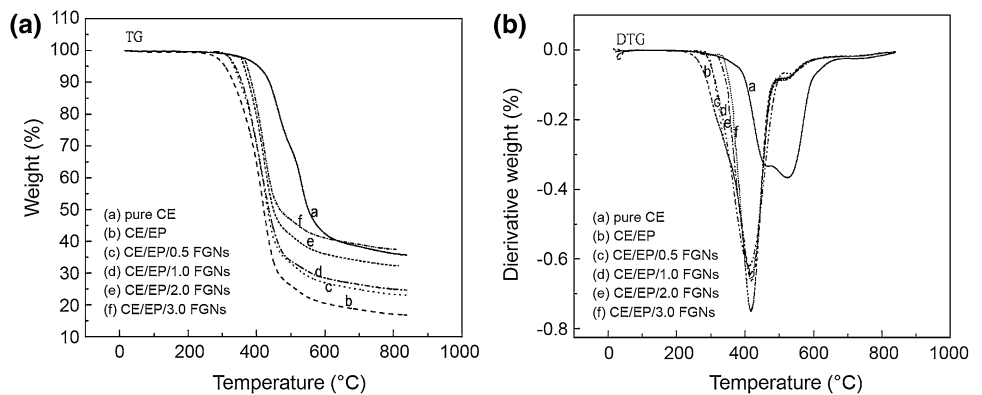


Table 1 Characteristic temperatures of FGNs/CE/EP nanocomposites obtained from TG analysis

	Pure CE	CE/EP	CE/EP/0.5FGNs	CE/EP/1.0FGNs	CE/EP/2.0FGNs	CE/EP/3.0FGNs
$T_{5\%}$	289.8	254.2	297.2	300.6	282.6	289.0
T_{\max}	525.5	417.9	417.0	412.9	412.7	416.1
T_{final}	838.2	838.5	838.6	838.3	813.6	813.7

TG analysis

The thermal degradation behaviors of the pure CE resin, CE/EP copolymer and FGNs/CE/EP nanocomposites with different FGNs contents were evaluated by TG in combination with DTG analyses. The curves of TG and DTG are presented in Fig. 8a, b, respectively. The characteristic temperatures $T_{5\%}$, T_{\max} and T_{final} of the FGNs/CE/EP nanocomposites obtained from TG analysis are shown in Table 1. From Fig. 8a, the weight loss increases gradually from 300 to 600 °C and the nanocomposites show higher char residue than that of the CE/EP copolymer, but lower than that of pure CE resin. Thus, the addition of FGNs increases the thermal stability of the FGNs/CE/EP nanocomposites. This is because the macromolecular chain stability of the FGNs/CE/EP nanocomposites is enhanced by the interfacial bonding between the FGNs and the matrix. Figure 8b shows that the thermal degradation temperatures

corresponding to the peaks enhance slowly with increasing the FGNs content. The thermal degradation temperatures of the FGNs/CE/EP nanocomposites are higher than that of the CE/EP copolymer, but lower than that of pure CE resin as well. These phenomena indicate that the addition of FGNs improves the thermal stability of the FGNs/CE/EP nanocomposites.

Conclusion

Functional graphene nanoflakes were employed as fillers to improve the integrated properties of the FGNs/CE/EP nanocomposites. The results described that the FGNs/CE/EP nanocomposites with appropriate FGNs contents had excellent comprehensive properties. The flexural and impact strength of the FGNs/CE/EP nanocomposites with 2.0 wt% FGNs content reached 170.8 MPa and 15.5 kJ/

m^2 , respectively. The dielectric and thermal properties of the FGNs/CE/EP nanocomposites with 2.0 wt% FGNs increased as well. Therefore, the incorporation of the FGNs into the CE/EP copolymer had a significant effect in improving the physical and chemical properties of the nanocomposites. The FGNs acted not only as a catalyst in the whole curing process, but also as a reinforcing agent in the FGNs/CE/EP nanocomposites.

References

- Novoselov KS, Geim AK, Morozov SV, Jiang D, Zhang Y, Dubonos SV, Grigorieva IV, Firsov AA (2004) Electric field in atomically thin carbon films. *Science* 306:666–669
- Mo ZL, Liu PW, Guo RB, Deng ZP, Zhao YX, Sun Y (2012) Graphene sheets/Ag₂S nanocomposites: synthesis and their application in super capacitor materials. *Mater Lett* 68:416–418
- Li YQ, Pan DY, Chen SB, Wang QH, Pan GQ, Wang TM (2013) In situ polymerization and mechanical, thermal properties of polyurethane/graphene oxide/epoxy nanocomposites. *Mater Des* 47:850–856
- Han DL, Yan LF, Chen WF, Li W (2011) Preparation of chitosan/graphene oxide composite film with enhanced mechanical strength in the wet state. *Carbohydr Polym* 83:653–658
- Kim H, Abdala AA, Macosko CW (2010) Graphene/polymer nanocomposites. *Macromolecules* 43:6515–6530
- Lee CG, Wei XD, Kysar JW, Hone J (2008) Measurement of the elastic properties and intrinsic strength of monolayer graphene. *Science* 321:385–388
- Lin Y, Song M, Stone CA, Shaw HJ (2013) A comprehensive study on the curing kinetics and network formation of cyanate ester resin/clay nanocomposites. *Thermochim Acta* 552:77–86
- Shi XD, Gan ZH (2007) Preparation and characterization of poly(propylene carbonate)/montmorillonite nanocomposites by solution intercalation. *Eur Polym J* 43:4852–4858
- Rodgers RM, Mahfuz H, Rangari VK, Chisholm N, Jeelani S (2005) Infusion of SiC nanoparticles into SC-15 epoxy: an investigation of thermal and mechanical response. *Macromol Mater Eng* 290:423–429
- Zhou H, Chen Y, Fan HJ, Shi HH, Shi B (2008) The polyurethane/SiO₂ nano-hybrid membrane with temperature sensitivity for water vapor permeation. *J Membr Sci* 318:71–78
- Chen SB, Wang QH, Wang TM (2012) Damping, thermal, and mechanical properties of carbon nanotubes modified castor oil-based polyurethane/epoxy interpenetrating polymer network composites. *Mater Des* 38:47–52
- Abdalla M, Dean D, Robinson P, Nyairo E (2008) Cure behavior of epoxy/MWCNT nanocomposites: the effect of nanotube surface modification. *Polymer* 49:3310–3317
- Ramanathan T, Stankovich S, Dikin DA, Liu H, Shen H, Nguyen ST, Brinson LC (2007) Graphitic nanofillers in PMMA nanocomposites—an investigation of particle size and dispersion and their influence on nanocomposite properties. *J Polym Sci Part B Polym Phys* 45:2097–2112
- Kumar M, Chung JS, Kong BS, Kim EJ, Hur SH (2013) Synthesis of graphene-polyurethane nanocomposite using highly functionalized graphene oxide as pseudo-crosslinker. *Mater Lett* 106:319–321
- Chiu FC, Huang IN (2012) Phase morphology and enhanced thermal/mechanical properties of polyamide 46/graphene oxide nanocomposites. *Polym Test* 31:953–962
- Patole AS, Patole SP, Jung SY, Yoo JB, An JH, Kim TH (2012) Self-assembled graphene/carbon nanotube/polystyrene hybrid nanocomposite by in situ microemulsion polymerization. *Eur Polym J* 48:252–259
- Kuilla T, Bhadra S, Yao D, Kim NH, Bose S, Lee JH (2010) Recent advances in graphene based polymer composites. *Prog Polym Sci* 35:1350–1375
- Liu M, Duan YX, Wang Y, Zhao Y (2014) Diazonium functionalization of graphene nanosheets and impact response of aniline modified graphene/bismaleimide nanocomposites. *Mater Des* 53:466–474
- Wang YQ, Kou KC, Wu GL (2015) Effect of bisallylbenzoxazine on the thermal, mechanical and dielectric properties of bismaleimide-cyanate blend polymer. *RSC Adv* 5:58821–58831
- Wu GL, Cheng YH, Xie Q, Liu C, Kou K, Zhuo L, Wang Y (2014) Synthesis of a bismaleimide/cyanate ester copolymer containing phenolphthalein functional group with excellent dielectric properties and thermally stable. *J Polym Res* 21:615–622
- Wang X, Xing WY, Zhang P, Song L, Yang H, Hu Y (2012) Covalent functionalization of graphene with organosilane and its use as a reinforcement in epoxy composites. *Compos Sci Technol* 72:737–743
- Szeluga U, Kumanek B, Pusz S, Czajkowska S (2015) Preparation and characterization of carbon foams derived from cyanate esters and cyanate/epoxy copolymers. *J Therm Anal Calorim* 122:271–279
- Sudha JD, Pradhan S, Viswanath H, Unnikrishnan J, Brahmabhatt P, Manju MS (2014) Studies on the cure parameters of cyanate ester-epoxy blend system through rheological property measurements. *J Therm Anal Calorim* 115:743–750
- Lin QL, Qu LJ, Lü QF, Fang C (2013) Preparation and properties of graphene oxide nanosheets/cyanate ester resin composites. *Polym Test* 32:330–337
- Wang X, Jin J, Song M (2012) Cyanate ester resin/graphene nanocomposite: curing dynamics and network formation. *Eur Polym J* 48:1034–1041
- Bai H, Xu YX, Zhao L, Li C, Shi G (2009) Non-covalent functionalization of graphene sheets by sulfonated polyaniline. *Chem Commun* 45:1667–1669
- Duan JK, Shao SX, Li Y, Wang LF, Jiang PK, Liu BP (2012) Poly(lactide)/graphite nanosheets/MWCNTs nanocomposites with enhanced mechanical, thermal and electrical properties. *Iran Polym J* 21:109–120
- Mi YN, Liang GZ, Gu AJ, Zhao F, Yuan L (2013) Thermally conductive aluminum nitride—multiwalled carbon nanotube/cyanate ester composites with high flame retardancy and low dielectric loss. *Ind Eng Chem Res* 52:3342–3353
- Lin CH, Huang SJ, Wang PJ, Lin HT, Dai SA (2012) Miscibility, microstructure, and thermal and dielectric properties of reactive blends of dicyanate ester and diamine-based benzoxazine. *Macromolecules* 45:7461–7466
- Jiang DY, Zhou Q, Fan Q, Ni LZ (2015) Curing behavior and thermal performance of cyanate ester resin modified by poly(methyl-benzene diethynylbenzene) silane. *Polym Bull* 72:2201–2214
- Han CF, Gu AJ, Liang GZ, Yuan L (2010) Carbon nanotubes/cyanate ester composites with low percolation threshold, high dielectric constant and outstanding thermal property. *Compos A* 41:1321–1328
- Blasi CD, Branca C, Galgano A, Moricone R, Milella E (2009) Oxidation of a carbon/glass reinforced cyanate ester composite. *Polym Degrad Stab* 94:1962–1971
- Kissoukko DA, Deitzel JM, Doherty SP, Shah A, Gillespie JW (2008) Understanding the role of clay silicate nanoparticles with organic modifiers in thermal curing of cyanate ester resin. *Eur Polym J* 44:2807–2819

34. Goertzen WK, Kessler MR (2007) Thermal and mechanical evaluation of cyanate ester composites with low-temperature processability. *Compos A* 38:779–784
35. Hummers WS Jr, Offeman RE (1958) Preparation of graphitic oxide. *J Am Chem Soc* 80:1339
36. Jafarkhani M, Fazlali A, Moztarzadeh F, Mozafari M (2012) Mechanical and structural properties of polylactide/chitosan scaffolds reinforced with nano-calcium phosphate. *Iran Polym J* 21:713–720